Molecular Crystals and Liquid Crystals Science and Technology. Section A. Molecular Crystals and Liquid Crystals

Publication details, including instructions for authors and subscription information:
http://www.tandfonline.com/loi/gmcl19

Poly(silylene)s: Effect of Polar Acceptor Side Groups on the Charge Carrier Photogeneration and Transport

Stanislav Nešpůrek [a b], Jiří Pfleger [a], Eduard Brynda [a], Ivan Kmínek [a], Andrey Kadashchuk [c], Alexander Vakhnin [c] & Juliusz Sworakowski [d]

[a] Institute of Macromolecular Chemistry, Academy of Sciences of the Czech Republic, Heyrovský Sq. 2, 162 06, Prague, 6

[b] Chemical Faculty, Technical University, Purkyňova 18, Brno, Czech Republic

[c] Institute of Physics, NASU, Prospekt Nauki 46, 252022, Kiev, Ukraine

[d] Institute of Physical and Theoretical Chemistry, Technical University of Wroclaw, Wyb. Wyspianskiego 27, 50-370, Wroclaw, Poland

Version of record first published: 24 Sep 2006

Mol. Cryst. Liq. Cryst., Vol. 355, pp. 191-216
Reprints available directly from the publisher
Photocopying permitted by license only

Poly(silylene)s: Effect of Polar Acceptor Side Groups on the Charge Carrier Photogeneration and Transport*

STANISLAV NEŠPŮREK[abt†], JIŘÍ PFLEGER[a], EDUARD BRYNDA[a], IVAN KMÍNEK[a], ANDREY KADASHCHUK[c], ALEXANDER VAKHNIN[c] and JULIUSZ SWORAKOWSKI[d]

[a]Institute of Macromolecular Chemistry, Academy of Sciences of the Czech Republic, Heyrovský Sq. 2, 162 06 Prague 6, [b]Chemical Faculty, Technical University, Purkyňova 18, Brno, Czech Republic, [c]Institute of Physics, NASU, Prospekt Nauki 46, 252022, Kiev, Ukraine and [d]Institute of Physical and Theoretical Chemistry, Technical University of Wroclaw, Wyb. Wyspianskiego 27, 50–370 Wroclaw, Poland

(Received December 03, 1999; In final form February 02, 2000)

The influence of polar electron-acceptor chromophores (both admixed and covalently bonded to the polymer backbone) on photoelectrical properties of poly[methyl(phenyl)silylene] was studied. Whereas the charge carrier mobility decreased for any concentration of the chromophore, the photogeneration efficiency increased for concentrations up to about 4 mole %. For higher concentrations, some decrease was observed. The decrease in mobility was ascribed to the electron-dipole interaction and to the broadening of the density-of-states distribution affecting the hopping transport.

Keywords: photoconductivity; charge transport; electron-dipole interaction; polysilylenes

INTRODUCTION

Poly(silylene)s have been extensively studied as a new class of photoconductors[1–3] and charge-transporting polymers[4,5] because of a high efficiency of charge photogeneration and charge carrier drift mobility of the order of 10^{-8} $m^2V^{-1}s^{-1}$, unusually high for polymeric materials. Of several poly(silylene)s

* Dedicated to the memory of Professor Edgar Silinsh

† Corresponding Author.

studied to date, much information has been accumulated for poly[methyl(phenyl)silylene] (see Scheme 1), herein referred to as PMPSi.

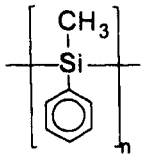

PMPSi

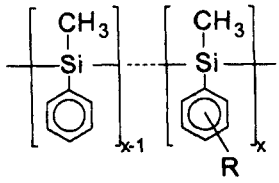

–R:

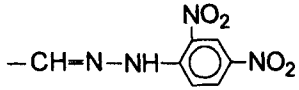

PMPSi-DNPH

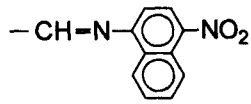

PMPSi-NNI

Additives:

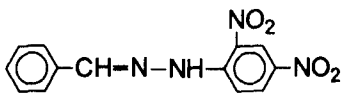

BDNPH

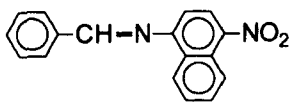

BNNI

SCHEME 1

The charge carrier photogeneration in poly(silylene)s associated with excitation of the σ-conjugated electron system of the polymer backbone is limited to the UV spectral range. These excitations are, among others, accompanied by gradual photodegradation of the polymer by the homolytic main-chain scission.[6] The UV photodegradation can considerably be decreased by π-conjugated substituents and dopants whose absorption overlaps the emission band of PMPSi.[7] At the same time, some of these substituents bonded to the phenyl

group, such as (2,4-dinitrophenylhydrazono)methyl (DNPH) or [(4-nitro-1-naphthyl)imino]methyl (NNI), shift the spectral region of the charge photogeneration outside the σ-σ* absorption to wavelengths longer than 360 nm.[8] In addition to the increased photogeneration efficiency in the region of σ-σ* transitions (335 nm), the charge carriers could also be generated in the spectral region of the chromophore absorption around 400 nm with the quantum efficiency comparable with that of the photogeneration originated in the σ-system of unmodified PMPSi.[9] A similar effect of the increase in the quantum efficiency of the charge carrier photogeneration was achieved by addition of low-molecular-weight acceptor dopants.[10,11] However, substitution of PMPSi with chromophores at a degree above 10 mole % (as was done in the previous work) resulted in a dramatic decrease in the charge carrier mobility in these polymers, accompanied by an increase in the dispersivity of the transport.[8] Thus, chemical substitution or a "physical" doping of polymeric photoconductors is a complex effect involving, among others, an increase in the dispersivity of the charge carrier transport by polar additives and charge carrier trapping. To better understand these processes, we studied photoelectrical properties of two derivatives of PMPSi containing polar electron-acceptor chromophores:

(i) poly[methyl(phenyl)silylene/{3(4)-[(2,4-dinitrophenylhydrazono) methyl]phenyl} methylsilylene] (PMPSi-DNPH),

(ii) poly[methyl(phenyl)silylene/methyl(3(4)-{[*N*-(4-nitro-1-naphthyl)imino]methyl}phenyl)silylene] (PMPSi-NNI).

For comparison, model systems consisting of PMPSi with admixed low-molecular-weight-chromophores:

(i) benzaldehyde 2,4-dinitrophenylhydrazone (BDNPH),

(ii) benzaldehyde *N*-(4-nitro-1-naphthyl)imine (BNNI)

were also studied (see Scheme 1 for all the chemical formulas).

EXPERIMENTAL

Materials

PMPSi (see Scheme 1) was prepared by sodium-mediated Wurtz coupling polymerization as described by Zhang and West.[12] The low-molecular-weight fraction was extracted with boiling diethyl ether. The residual polymer, obtained in ca. 17 % yield, possessed an unimodal but broad molar mass distribution, $M_w = 4\times10^4$ gmol^{-1}.

Copolymers PMPSi-DNPH and PMPSi-NNI were obtained by the following multistep process:

The parent PMPSi was chloromethylated with a mixture of chloromethyl methyl ether and $SnCl_4$ in dry chloroform using the procedure described elsewhere.[13] The degree of the chloromethylation was controlled by the concentration of chloromethyl methyl ether, temperature and reaction time. Quarternization of the resulting product yielding the pyridinium salt was accomplished by heating the chloromethylated polymer in boiling ethanol/pyridine mixture. Subsequently, most of the solvent was removed on a rotary evaporator and the product was precipitated by addition of diethyl ether and reprecipitated from ethanol solution with diethyl ether. The conversion in this step was nearly 100 %.

In the following step the pyridinium salt of PMPSi underwent the Kroehnke reaction with 4-nitroso-*N,N*-dimethylaniline and sodium methoxide in tetrahydrofuran (THF) or THF/methanol. Subsequently, the reaction mixture was poured into an excess of water saturated with NaCl. The precipitated polymer was filtered off, washed thoroughly with water, dried and reprecipitated into an excess of hexane. As a result, a brownish-yellow powder was obtained in the yield of 73 %. This polymer was further acid-hydrolysed in a THF solution with HCl added. The product was washed with water, dried and reprecipitated twice from THF solution with methanol. The yield was about 87 %. The resulting white powder consisting of PMPSi having some phenyl rings substituted with -CH=O groups was used as a starting polymer (PMPSi-CHO) for preparation of both the copolymers under study.

The PMPSi-DNPH polymer (with various degrees of substitution ranging between 0.55 and 15 %) was prepared by addition of 2,4-dinitrophenylhydrazine in aqueous $HClO_4$ to a solution of the starting polymer PMPSi-CHO in THF. The polymer PMPSi-NNI (containing 15 % of substituted phenyl groups) was prepared by the same procedure using 4-nitro-1-naphthylamine instead of 2,4-dinitrophenylhydrazine. Both polymers were filtered off and precipitated twice from THF solution with methanol before further physical studies. Using size-exclusion chromatography, the molar mass was determined to be $M_w = 1.9\times10^4$ $gmol^{-1}$ for PMPSi-DNPH and $M_w = 1.5\times10^3$ $gmol^{-1}$ for PMPSi-NNI (both at the degree of substitution 15 %).

The low-molecular-weight additive BDNPH was prepared by boiling benzaldehyde with 2,4-dinitrophenylhydrazine and p-toluenesulphonic acid in toluene for 30 min and purified by recrystallization. BNNI was prepared in a similar way using 4-nitro-1-naphthylamine instead.

Polymer films for photoconductivity measurements were prepared by spin casting a toluene solution of polymers on conductive ITO glass or glass covered

with a semitransparent Au electrode. The thickness of the films ranged from 3 to 5 μm. The polymers were reprecipitated three times from toluene solution with methanol. The toluene solution was then centrifuged (12 000 rpm, 15 min) before thin film preparation. After deposition the films were dried at 0.1 Pa and at 330 K for at least 4 h. The top Al electrode, 40 – 60 nm thick, was deposited by vacuum evaporation. Samples for thermostimulated luminescence (TSL) measurements were prepared in a similar way on stainless steel substrates.

Photocurrent Measurements

Photocurrent measurements were performed by the time-of-flight technique. The electrical circuit consisted of a voltage source, sample and oscilloscope (Hewlett-Packard model 54510 A, 50 Ω input impedance), connected in series. The samples were irradiated through a transparent ITO or semitransparent Au electrode with 347 nm single laser pulses (duration 20 ns) generated by a ruby laser (Korad model K1QS2) operated in conjunction with a frequency doubler. The penetration depth of the light was 0.13 μm corresponding to less than 4 % of the sample thickness. All measurements were made in vacuo at 10^{-4} Pa or in argon atmosphere. During the measurements, the samples were mounted in a cryostat and kept at a constant temperature with the accuracy of ± 0.2 K. The intensity of the excitation pulses was kept as low as possible to keep materials unchanged during the measurement. No photodegradation of the polymers was detected by measuring UV-VIS absorption spectra of the films after the photoconductivity measurements.

The charge carrier mobility was calculated from the relationship $\mu = L/(t_0 F)$, where L is the sample thickness, F is the electric field strength, and t_0 stands for the effective transit time. The effective transit times were determined from the intersection point of asymptotes to the pre-transient and post-transient sections of the photocurrent traces. Whenever the cusps on transient currents were well defined, interpolation was made using the curves plotted in linear co-ordinates, whereas in the case of ill-defined transit times (at higher chromophore concentrations) indicating a dispersive transport, their position was determined from the intersection of transient currents plotted in the log(current) vs. log(time) coordinates.[14] The transit time defined in such a way slightly differs from the "exact" average transit time t_r, as was shown by Monte Carlo simulation studies.[15] However, within the limit of experimental error, dependences of the mobility on temperature and electric field strength could be determined properly in this way. Over the range of temperatures and electric field strengths investigated, temperature and field dependences of the mobility were reproducible, with no indications of hysteresis.

The current transients were numerically integrated to obtain a total photogenerated charge in the sample. The quantum photogeneration efficiency was calculated from the total charge and photon flux.

Thermostimulated Luminescence

Thermostimulated luminescence (TSL) measurements were carried out with a laboratory-made apparatus for optical thermoactivated spectroscopy, covering the temperature range 4.2–350 K with an accuracy of 0. 1 K. Polymer samples were mounted in a holder of an optical helium cryostat and, after cooling down to 4.2 K, irradiated with UV light using a highpressure 500 W mercury lamp. The heating rate during all TSL runs was 0.15 Ks^{-1}. The TSL signal was detected with a cooled photomultiplier operated in the photon-counting mode. The TSL technique and the procedure of data processing were similar to those described previously.[16–19]

RESULTS

Undoped PMPSi

A typical transient current trace measured in a thin film of unmodified PMPSi is shown in Figure 1, curve 1. After a laser flash, the photocurrent rises abruptly reaching a plateau followed by a tail; the shape of the tail is related to a velocity dispersion within the carrier package drifting through the film. The tail-broadening parameter $w = (t_{1/2} - t_0)/t_{1/2}$ (where time t_0 is defined in the way described in the preceding section and $t_{1/2}$ is the time required for the current to decay to one-half of the "plateau" value) is only slightly dependent on the electric field strength, but strongly temperature-dependent (see Figure 2). Figure 3 illustrates the $\mu(F)$ dependences at various temperatures. In all cases, the mobility can be described by an $\exp(\beta F^{1/2})$ dependence for $F > 10^7$ Vm^{-1}, whereas at lower fields, $\mu(F)$ was found constant or a decreasing function of F. This behaviour is in agreement with the data published by Bässler et al.,[4] but at variance with the data of Abkowitz et al.[20] who reported the $\exp(\beta F^{1/2})$ law extending over two decades down to $F = 10^6$ Vm^{-1}. Regarding the temperature dependence of the mobility (see Figure 4), a linear dependence of $\ln\mu$ on $1/T^2$ was found for temperatures lower than $T_g = 408$ K (glass transition temperature).

Figure 5 (curve 1) shows the electric field dependence of the charge carrier photogeneration efficiency for sandwich cell ITO/PMPSi/Al. The behaviour,

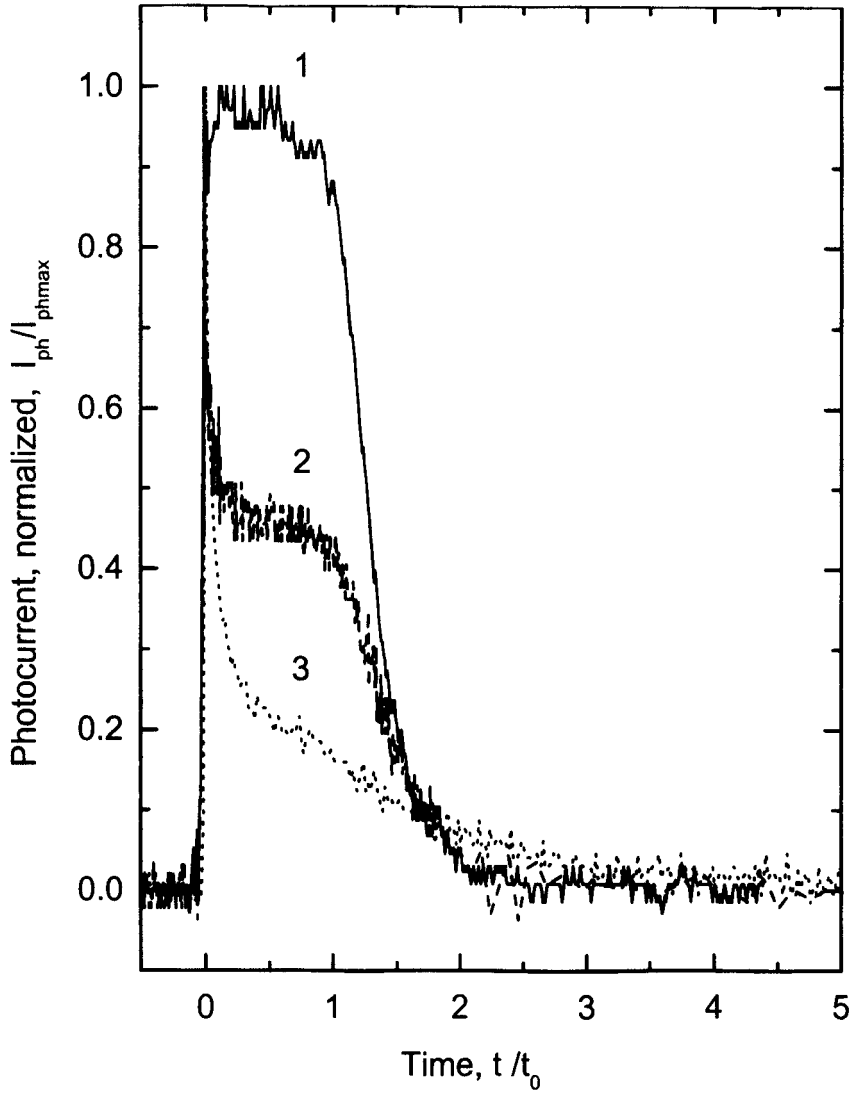

FIGURE 1 Typical photocurrent transients: Curve 1 – PMPSi, curve 2 – PMPSi-DNPH (substitution degree 0.88 mole %), curve 3 – PMPSi-DNPH (substitution degree 10 mole %). The curves are presented in the relative coordinates: currents have been normalized to their peak values and time to the transit times

namely the increase in the efficiency followed by saturation at higher values of the electric field, is similar to that observed by Kepler et al.[21] and can be inter-

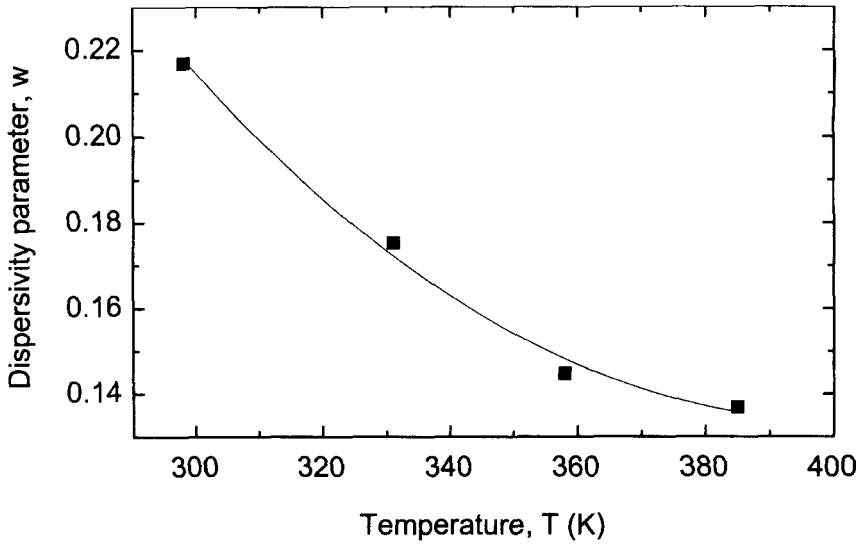

FIGURE 2 Dependence of the dispersion parameter w on temperature for PMPSi films

preted in terms of inelastic scattering of the photogenerated charge carriers in the region of a precontact potential barrier and in terms of trapping of the carriers in surface traps.[22]

Figure 6 (curve 1) presents a typical TSL curve measured on a PMPSi film. It shows an asymmetric broad peak with a maximum at T_m= 90 K; its low temperature portion being broader than the high-temperature one. This behaviour, predicted by the theory,[23] follows from the relaxation of ensemble of charge carriers before attaining a dynamic equilibrium. It was shown in our earlier work[19] that PMPSi exhibited a quasi-continuous trap distribution found by the fractional TSL[16–18] (the technique based on cycling the sample with a large number of small temperature oscillations superimposed on a constant heating ramp[16]). The mean activation energy $\langle E_a^{\Phi} \rangle$ can be determined during each temperature cycle as

$$\langle E_a^{\Phi} \rangle = -d[\ln \Phi(T)]/d(1/kT) \tag{1}$$

where Φ is the intensity of the thermoluminescence, T is the temperature in the measuring cycle, and k is the Boltzmann constant. The fractional TSL measurements[19] showed that the mean activation energy increases linearly with temperature according to the following empirical formula (in eV): $\langle E_a^{\Phi} \rangle(T) = 0.0028T - 0.05$. Taking into consideration the theory of the frac-

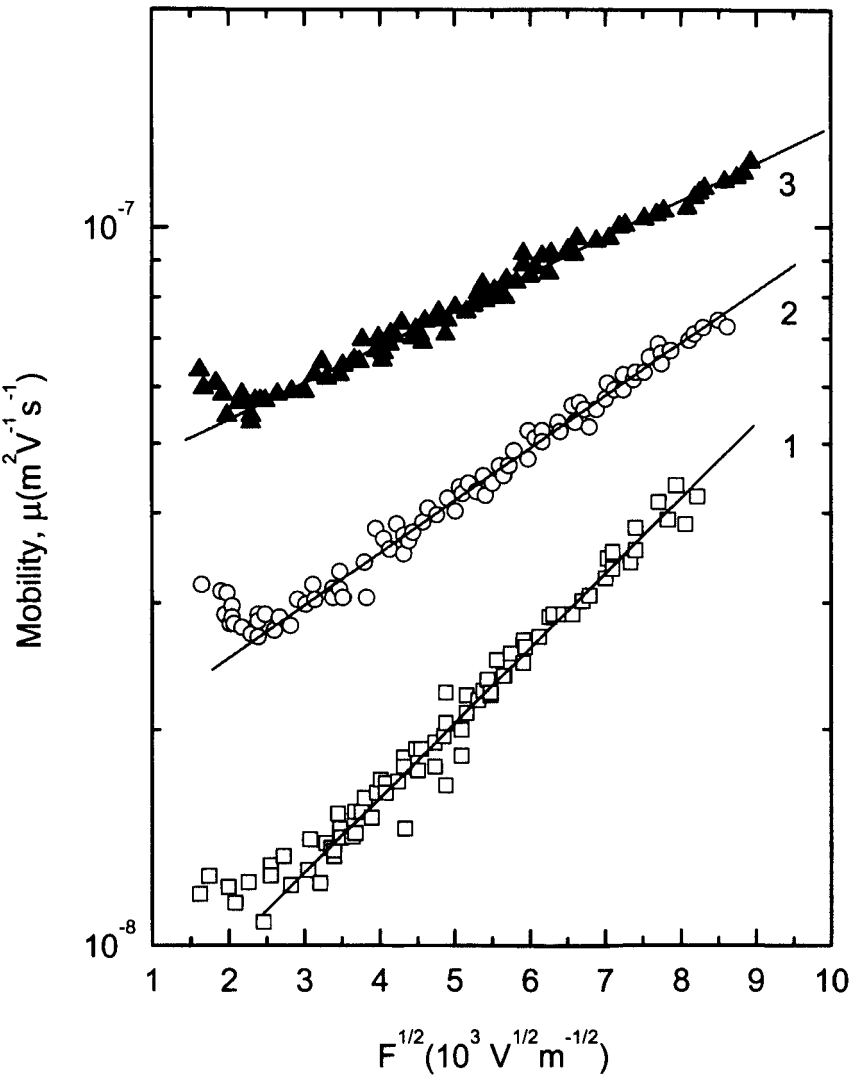

FIGURE 3 Dependence of charge carrier mobility of PMPSi on electric field strength, parametric in temperature. T = 295, 325, and 355 K for curves 1 – 3, respectively

tional TSL[16–18] and the above linear dependence for $\langle E_a^{\Phi} \rangle(T)$, and assuming that the TSL peak is associated with the thermal release of charge carriers occupying the intrinsic tail states, the temperature profile of the TSL peak directly reflects the distribution function of local states filled with charge carriers. For

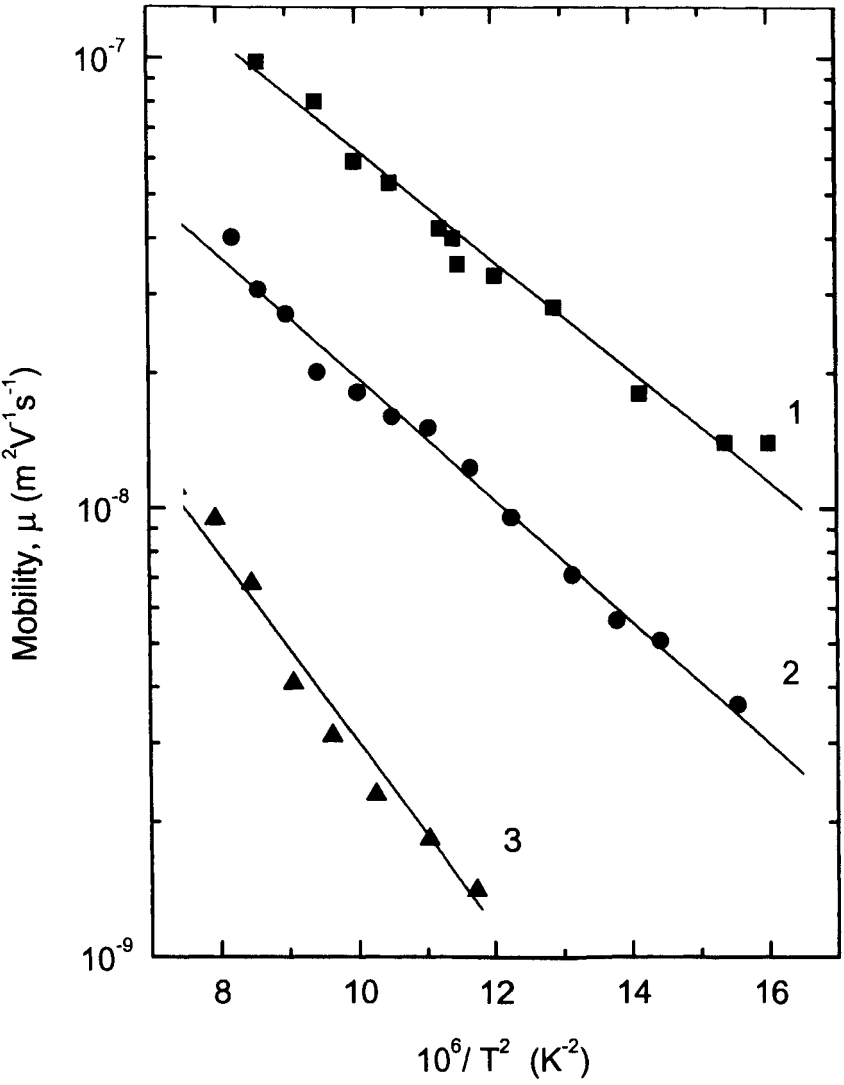

FIGURE 4 Temperature dependence of the hole mobility measured at the biasing electric field of 5×10^7 Vm^{-1}. Curve 1, PMPSi; curve 2, PMPSi-DNPH (substitution degree 0.88 mole %); curve 3, PMPSi-DNPH (substitution degree 10 mole %)

sufficiently deep states, this distribution function can be taken to be identical to the density-of-states (DOS) function $\rho(E)$. The temperature scale can be converted into the trap energy scale in a way similar to that described by

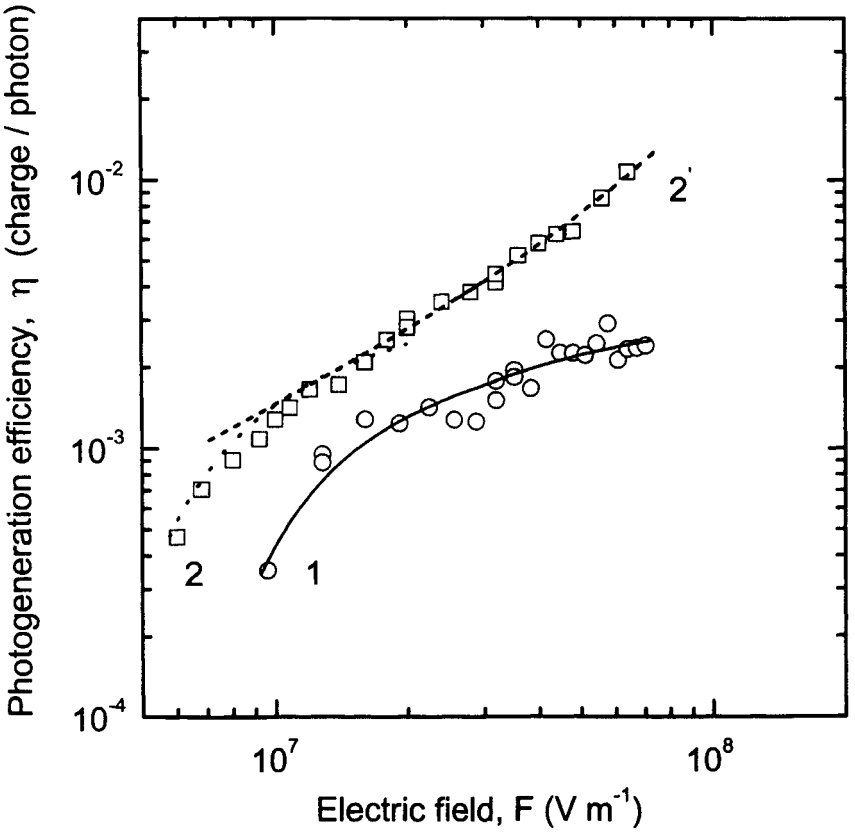

FIGURE 5 Field dependence of the photogeneration efficiency. Excitation wavelength 347 nm, T = 293 K: Circles and curve 1, PMPSi; squares and curves 2 and 2′, PMPSi-DNPH (substitution degree 1.1 mole %)

Bässler[24]and Eiermann et al.[25] for thermostimulated electrical currents. The high-temperature wing of the TSL peak could be well approximated by the following Gaussian function (cf. Figure 7)

$$\Phi_{TSL}(E) \sim \exp(-E^2/2\sigma^2) \qquad (2)$$

where E is the energy and σ is the half-width of the distribution of the transport hopping states. Using this approach, the value σ= 0.094 eV was obtained for PMPSi.

Figure 8 shows photocurrent transients in PMPSi for various levels of photon flux in the laser flash. For higher light intensities, the transients show a typical space-charge-limited behaviour[26]: after an initial spike, the current rises to a

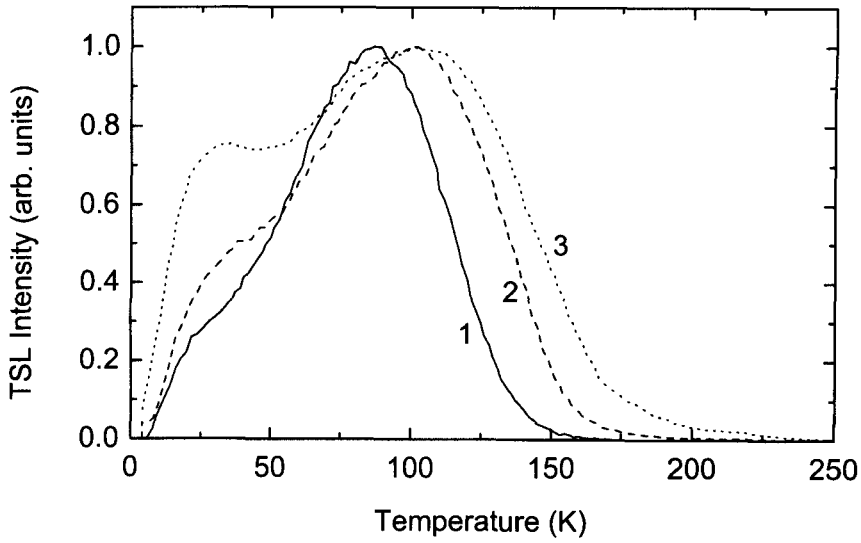

FIGURE 6 TSL glow curves recorded after excitation of the samples with unfiltered light of an Hg lamp at 4.2 K. Curve 1, PMPSi; curve 2, PMPSi doped with BNNI, 0.9 mole %; curve 3, PMPSi doped with BDNPH, 1.1 mole %

maximum occurring at a time t_{SCL}, which is ca. 20% shorter than the space-charge-free transit time t_0 observed at the same voltage. The apparent photogeneration efficiency decreased with increasing photon flux (see inset of Figure 8). This feature could be associated with a fast charge recombination, exciton quenching at the illuminated surface or an exciton-exciton annihilation.[27] However, the initial spike appearing in the photocurrent at high excitation light pulse intensities supports the explanation invoking a bimolecular recombination of mobile holes with trapped electrons in the vicinity of the illuminated electrode.

PMPSi-DNPH

Optical absorption spectra of the polymer PMPSi-DNPH, of the low-molecular-weight chromophores BDNPH and BNNI, and of a mixture of PMPSi with BNNI in toluene solutions are shown in Figure 9. Neither the position of the PMPSi absorption band at 335 nm nor the position of DNPH absorption band at 380 nm changed when the chromophore was covalently bonded to PMPSi. The absorption spectra of polymer films were similar to the solution spectra.

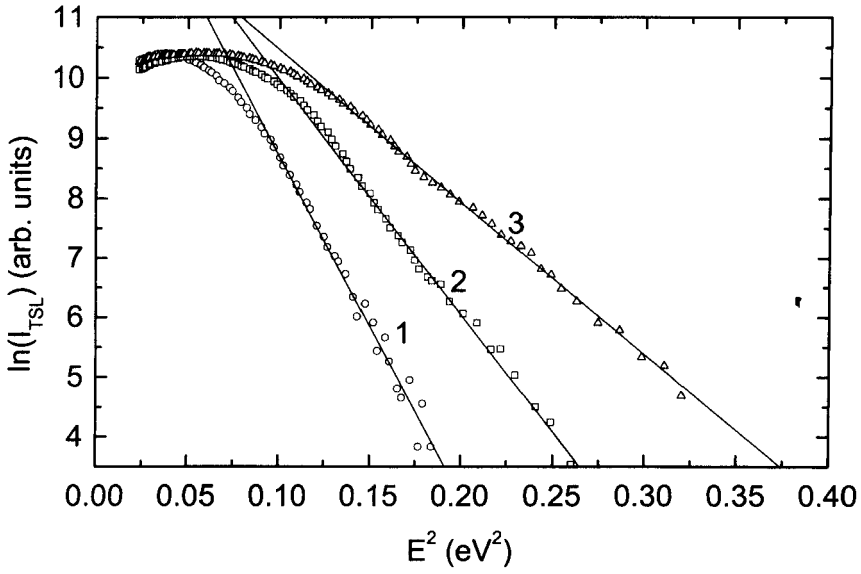

FIGURE 7 Gaussian analysis of the high-energy wings of the TSL peak according to Eq. (2) for the same materials as those shown in Figure 6

The presence of the acceptor groups substantially decreased the luminescence: the intensity of the emission peak at 360 nm, characteristic of PMPSi, dropped by one order of magnitude even at concentrations as low as 1 mole %, both for the chemically bonded groups and for the low-molecular-weight chromophores admixed to the polymer. It should also be mentioned that it was not possible to study TSL in polymers with the bonded side groups because of weak signal even for a low concentration of chromophore groups (c = 0.65 mole %).

Typical photocurrent transients expressed in normalised linear coordinates are shown in Figure 1. A well defined plateau, characteristic of unmodified PMPSi films (curve 1 in Figure 1), was also observed for the polymer with a low degree of substitution with DNPH (curve 2 in Figure 1). Substitution of 10 mole % in PMPSi-DNPH caused the transport to become dispersive (curve 3 in Figure 1). For all polymers with various concentrations of bonded side groups, measurable photocurrent transients were obtained only when the illuminated electrode was positively biased. This suggests that only holes were the mobile charge carriers. Figure 10 shows field dependences of the charge carrier mobility, parametric in temperature, for polymer PMPSi-DNPH with degree of substitution of 0.88 mole %. The characteristics are similar to those obtained for PMPSi (cf. Figure 3), the mobilities, however, being about one order of magnitude lower. A

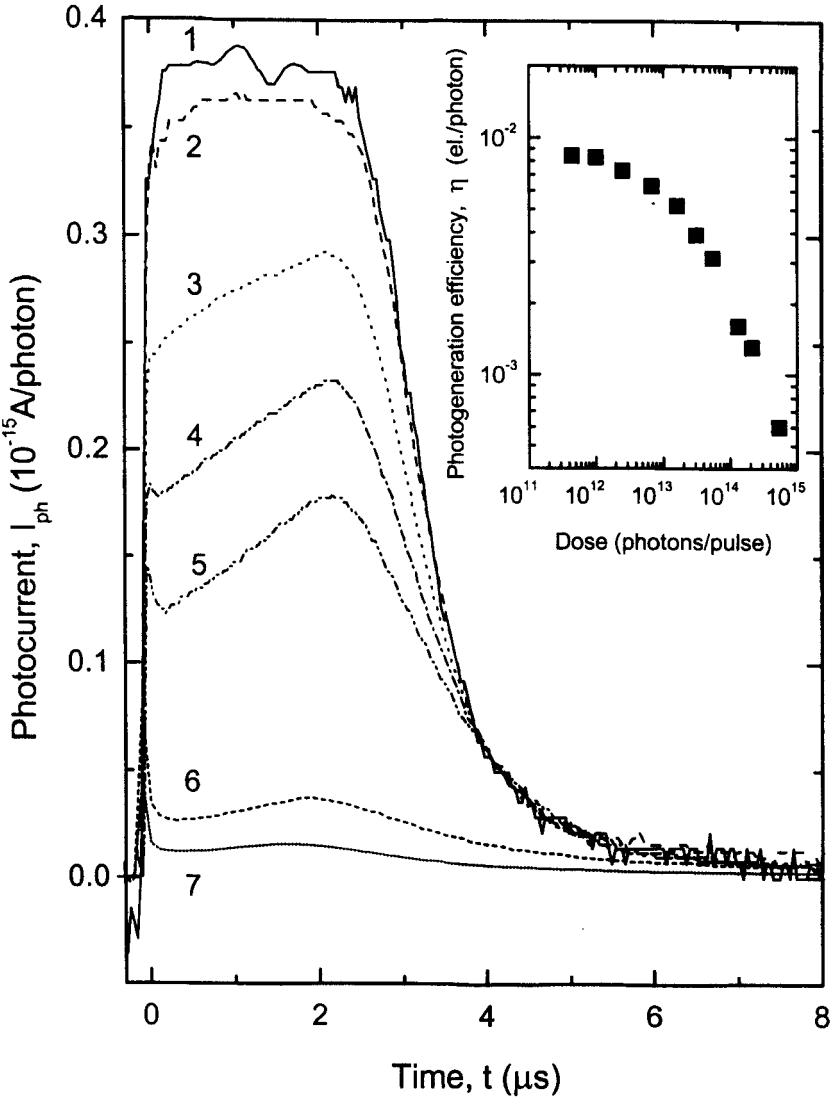

FIGURE 8 Photocurrent transients in PMPSi measured at various intensities of the laser flash: $\phi = 4.4 \times 10^{11}$ photon per flash, (curve 1), 1.0×10^{12} (curve 2), 6.8×10^{12} (curve 3), 1.6×10^{13} (curve 4), 3.1×10^{13} (curve 5), 2.1×10^{14} (curve 6), 5.4×10^{14}(curve 7). Inset: Dependence of the apparent photogeneration efficiency on photon flux

decrease in the mobility with the increasing electric field strength at low fields was followed by the mobility increase following the $\exp(\beta F^{1/2})$ dependence at higher fields. A similar behaviour was also observed in PMPSi-DNPH polymer

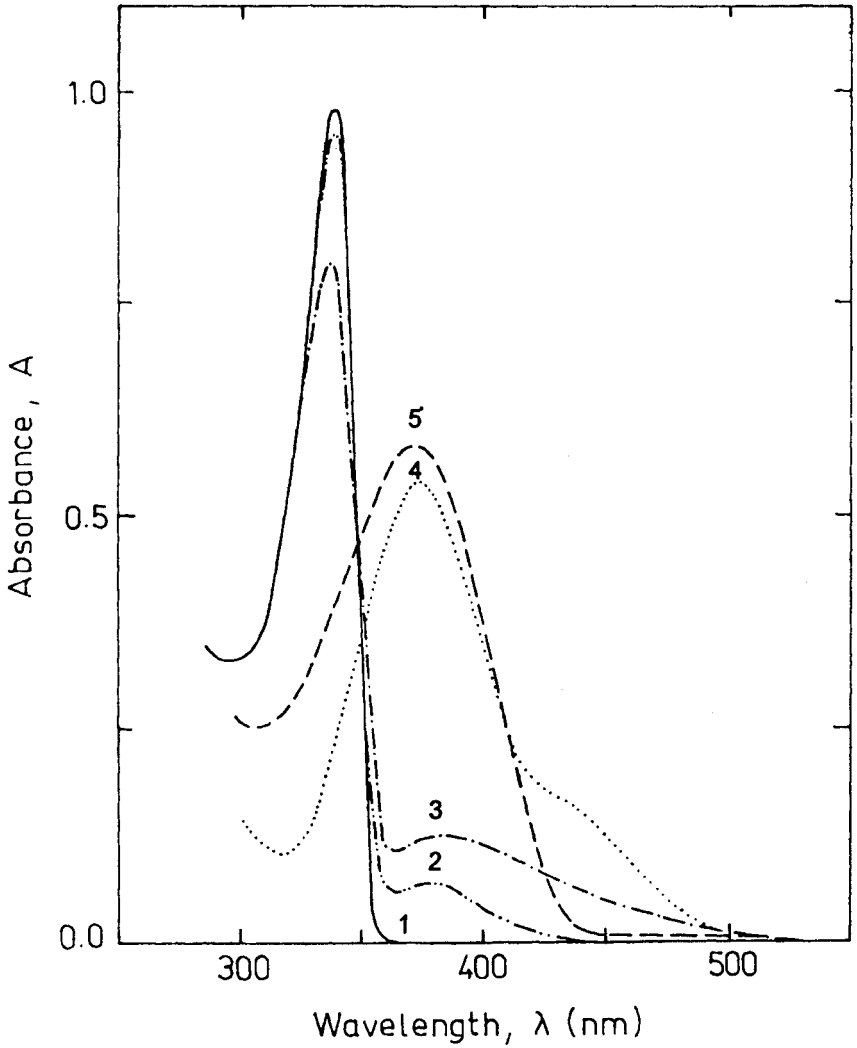

FIGURE 9 Optical absorption spectra of poly(silylene)s and chromophores in toluene solutions. Curve 1, PMPSi; curve 2, PMPSi mixed with 7 mole % of BNNI; curve 3, PMPSi-DNPH (substitution degree 10 mole %); curve 4, BDNPH (concentration 1.0×10^{-6}mol l^{-1}); curve 5, BNNI (5.9×10^{-6} mol l^{-1})

with degree of substitution of 0.55 and 1.29 mole %, whereas only a monotonic increase in the mobility with the field strength (without a decrease at low fields) was observed for the PMPSi-DNPH polymer with the degree of substitution of 10 mole %.

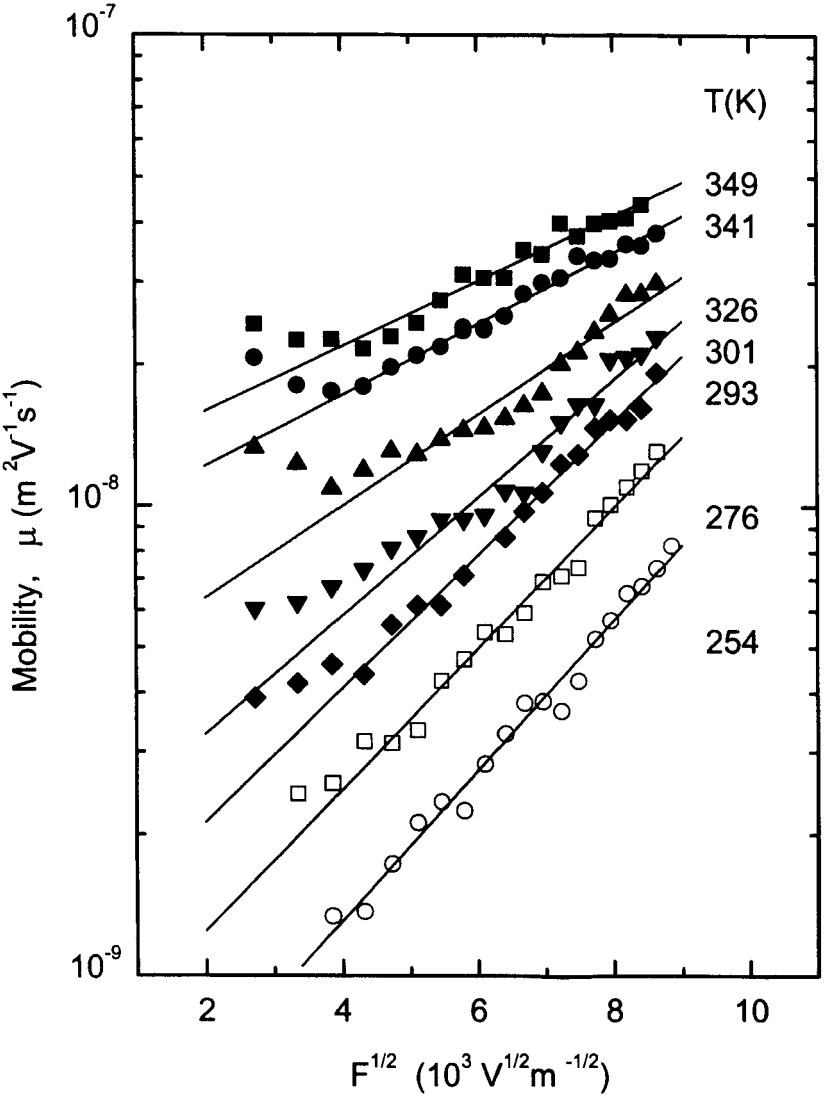

FIGURE 10 Field dependences of the hole mobility, parametric in temperature, for PMPSi-DNPH (substitution degree 0.88 mole %)

The temperature dependences of the hole mobility measured for PMPSi-DNPH with substitution degree 0.88 and 10 mole % at an electric field of $5 \times 10^7 \mathrm{Vm}^{-1}$ are plotted in Figure 4 as a logμ vs. T^{-2} coordinates (curve 2 and 3, respectively). Two facts should be mentioned comparing the μ vs. T^{-2} characteristics

for PMPSI-DNPH and PMPSi: (i) charge carrier mobility decreases with increasing concentration of chromophores; this dependence is given in Figure 11; (ii) the effective activation energy of the mobility (obtained from the Arrhenius plot) increases with increasing chromophore concentration. Here, a comment must be added: Usually it is difficult to experimentally distinguish between a $\mu(T^{-2})$ and a $\mu(T^{-1})$ dependence. An Arrhenius plot yields an apparent (effective) activation energy E^{μ}_{aeff} which is related to the width of the DOS function[15] (see below).

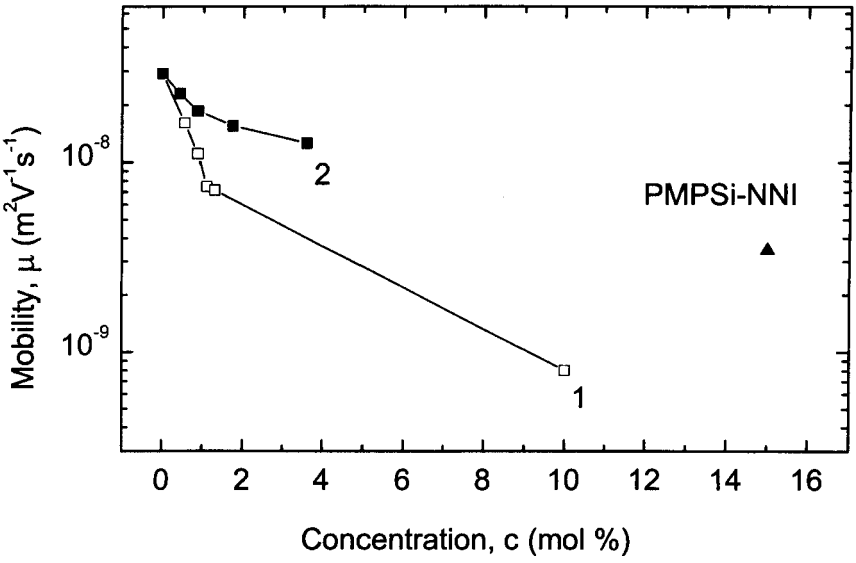

FIGURE 11 The dependences of the hole mobility on the concentration of the chromophore in PMPSi. Open squares and curve 1, PMPSi-DNPH polymer (λ = 347 nm, T = 293 K, biasing field F = 5×10^7 Vm^{-1}); closed squares and curve 2 – mixture of PMPSi with BNNI; for PMPSi-NNI polymer, only one point is available (triangle)

The effect of chromophore concentration on the photogeneration efficiency is shown in Figure 12. At low concentrations, the presence of chromophores in the polymer film increased the photogeneration efficiency; however, at chromophore concentration exceeding some 1 ÷ 3 mole %, the efficiency was found to decrease. The electric field dependence of the photogeneration efficiency measured in the PMPSi-DNPH polymer is presented in Figure 5 (squares and curves 2 and 2′). The shape of the dependence observed at low electric fields (Figure 5, curve 2) is similar to that of PMPSi without chromophores (curve 1 in Figure 5). A superlinear increase was observed with PMPSi-DNPH at the electric fields higher than 2×10^7 Vm^{-1} (Figure 5, curve 2′). The dashed line 2′ shows the fit according to the Onsager theory of geminate recombination.[28,29] It suggests

that acceptor-type side groups decrease the precontact barrier between the electrode and polymer and a nearly undistorted electric field dependence of the photogeneration efficiency can be obtained (similarly to the measurements with samples where a gas contact was applied[30] – xerographic photodischarge).

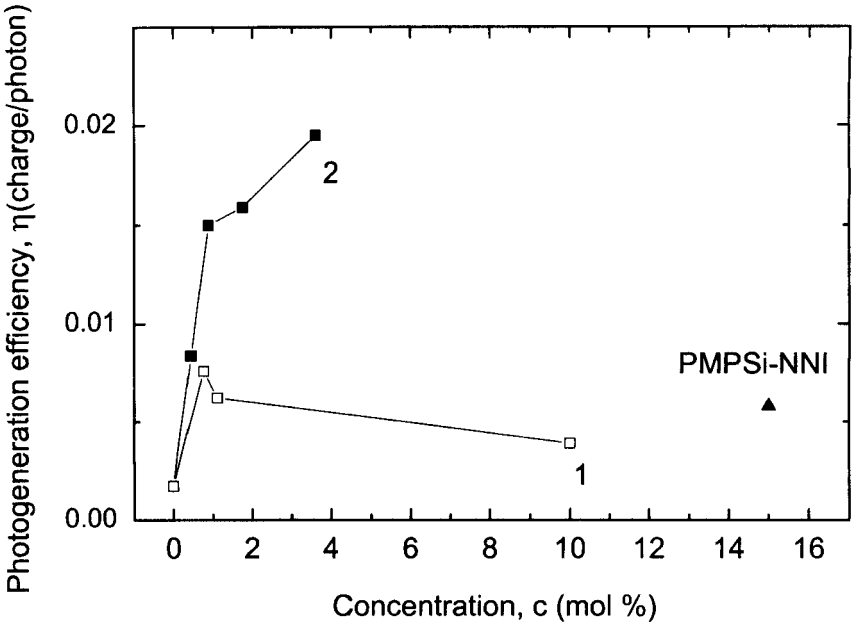

FIGURE 12 The dependence of the photogeneration efficiency on the chromophore concentration. ($\lambda = 347$ nm, $T = 293$ K, biasing field $F = 5\times 10^7$ V m^{-1}). (For the meaning of symbols, see Figure 11.)

PMPSi-NNI

Physical properties of this polymer were very similar to those of PMPSi-DNPH. Photocurrent transients showed a well defined plateau only at lower concentrations of the chromophore side groups, whereas for higher concentrations, the transport was dispersive with monotonic time decay of the photocurrent trace. The absolute value of the charge carrier mobility was lower than that of PMPSi, but higher than for the PMPSi-DNPH polymer (for comparable concentrations of the chromophore). As expected, this is in agreement with the dipole moments of side groups, 6 D and 7.6 D for BNNI and BDNPH, respectively, as calculated using the AM 1 and PM 3 quantum chemical methods.[31] The quantum generation efficiency was higher than for both PMPSi and PMPSi-DNPH. It should be

mentioned that the PMPSi-NNI polymer was photosensitive even in the spectral region above 400 nm, following an absorption spectrum of the chromophore (cf. Figure 9, curve 2). The photogeneration quantum efficiencies η of PMPSi and PMPSi-NNI, as obtained from xerographic measurements,[30] were at 254 nm $\eta = 0.010$ and 0.024, at 355 nm $\eta = 0.002$ and 0.012 charge per photon, respectively. At 405 nm, no photoelectrical sensitivity was detected for PMPSi, but $\eta = 0.005$ charge per photon was found for PMPSi-NNI. Thus, using suitable chromophore groups, one can make polysilylenes photosensitive even in visible spectral region.

Polymer Mixtures: PMPSi + BDNPH and PMPSi + BNNI

To study the influence of the chemical bonding of the chromophore to the polysilylene backbone on photoelectrical properties of the polymer, we performed comparative measurements on unmodified PMPSi containing corresponding low-molecular-weight chromophores, BDNPH and BNNI (cf. Scheme 1), admixed to the polymer. Unfortunately, for BDNPH only results for low concentrations of the dopant are available because the chromophore at higher concentrations tends to crystallize in the polymer host. One can state that photophysical behaviour of the mixtures is very similar to that of polymers with the same, but chemically bonded side groups. Optical absorption covers partly also the visible region, following the spectral curve of the chromophore (cf. curves 2 and 5 in Figure 9). The absorption spectra of doped polymer films prepared from solutions were similar to the solution spectra. The intensity of the sharp fluorescence emission peak at 360 nm decreased with increasing chromophore concentration. The character of the dependence was similar to that observed in the polymer with the chemically bonded groups. The photoelectrical behaviour was alike for both systems. Thus, we will only summarise the basic results: (i) The quantum photogeneration efficiency increased with increasing concentration of the dopant (Figure 3, curve 2) up to about 4 mole %. After that, usually a decrease was observed. This is in agreement with our measurement on the system PMPSi-NNI (cf. Figure 12, point labelled PMPSi-NNI). (ii) The charge carrier mobility decreases monotonically with increasing concentration of the dopant (cf. curve 2 in Figure 11) – this effect was attributed to the electron-dipole interaction and was discussed in detail elsewhere.[32] Both, increase of the dopant concentration and increase of the dipole moment result in broadening of the DOS function. It could be pointed out that similarly to the polymer with chemically bonded polar groups, the photocurrent transients showed a typical dispersive behaviour only for doping degrees higher than 10 mole %.

The influence of the dipole moment on the DOS function was studied by TSL. Figure 6 contains the glow curves for PMPSi (curve 1), for PMPSi + BNNI (0.9 mole %, curve 2) and for PMPSi + BDNPH (1.1 mole %, curve 3). All TSL curves in Figure 6 were monitored under the same conditions – UV excitation for 30 s at 4.2 K. Because the dopant concentrations were nearly the same for both cases, we could deduce the influence of the dipole moment of the dopant on the DOS function. As can be seen, the doping of PMPSi with BDNPH or BNNI led to a notable effect on the TSL glow curves of the doped samples, namely to a shift of TSL peak towards higher temperatures and to its broadening. It is evident that doping of PMPSi with both BDNPH and BNNI resulted in a notable increase in the energetic disorder due to the dipolar disorder contribution caused by polar additives. The TSL peak shift is larger for the BDNPH dopant. This effect might be explained by a larger dipole moment of BDNPH or/and formation of shallow traps (leading to a larger effective energetic disorder). Very probably both effects are operative simultaneously. The fractional TSL experiments showed that the temperature dependence of the mean activation energy, E_a^{Φ}, is essentially the same as in undoped PMPSi.[19]

The effect of polar additives can be seen more explicitly when comparing the TSL peaks obtained after an additional exposure of the samples to IR irradiation at 4.2 K (Figure 13). Generally, the effect of IR irradiation (IR filter transparency band was 900 – 4500 nm) on TSL was described in our previous works.[19,33,34] We explained the effect of the shift of the glow curve maximum to higher temperatures in terms of acceleration of energetic relaxation of photogenerated charge carriers within the Gaussian-shaped DOS. IR excitation to the higher energy portion of the DOS involves actually an increase in the number of new sites visited by a carrier at 4.2 K and, consequently, leads to an increase in the probability of reaching lower tail states. As can be seen from Figure 13, the TSL peak of doped PMPSi is notably shifted to higher temperatures as compared with undoped PMPSi.

Results of the Gaussian analysis of the high-temperature wing of TSL peaks are shown in Figure 7. The analysis was done just as described earlier,[19] i.e. by converting the temperature scale to the trap energy scale using the calibration expression mentioned above. As can be seen from Figure 7, the parameter σ, derived from the slopes of the lines, amounted to 0.11 eV for PMPSi + BNNI, i.e., it is larger than the value 0.094 eV determined for the undoped PMPSi. For PMPSi + BDNPH, the latter parameter was found equal to about $0.13 \div 0.14$ eV. It should be noted that these data might be slightly underestimated since we neglected the transport energy contribution.[19,33,34] From these results it is evident that the decrease in the charge carrier mobility due to doping the polymer with polar additives is associated with the electron-dipole interaction and the resulting broadening of the hopping states distribution.

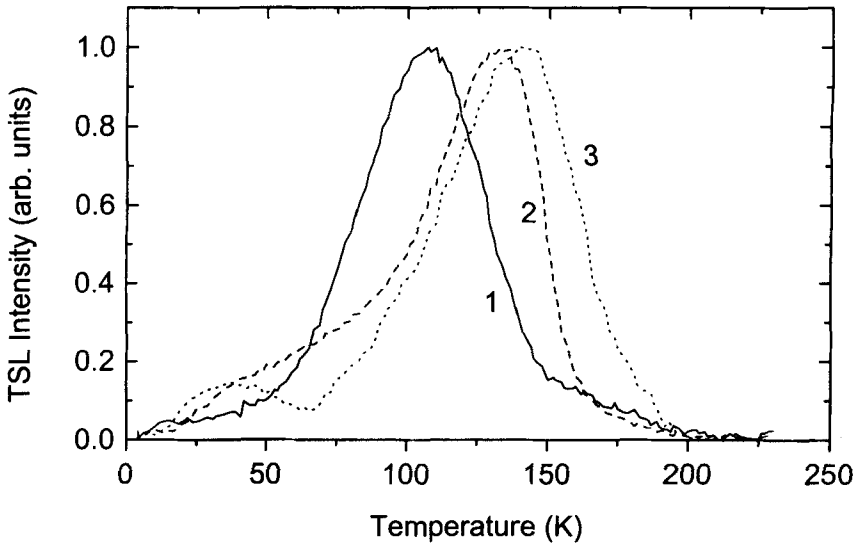

FIGURE 13 TSL glow curves measured for PMPSi (curve 1), PMPSi doped with BNNI, 0.9 mole % (curve 2), and PMPSi doped with BDNPH, 1.1 mole % (curve 3). Prior to the measurements, the samples were irradiated at 4.2 K with unfiltered light of an Hg lamp for 30 s, and subsequently with IR light for 30 min

As it was shown earlier, the disorder parameter, σ, could be evaluated from TSL data also by an alternative way, analysing the activation energy at the TSL peak maximum, $< E_{am}^{\Phi} >$. The following expression (3) was suggested (for details see Refs.[19,33,34]):

$$\sigma = \frac{< E_{am}^{\Phi} >}{[3 \ln \ln(t/t_{00})]^{1/2} - 1} \tag{3}$$

where t_{00} is the dwell time of a carrier at a lattice site without disorder (for a charge carrier, t_{00} is accepted to be 10^{-13}s).[35] It presumes a linear relationship between the experimentally accessible $< E_{am}^{\Phi} >$ and the degree of the energetic disorder in amorphous systems. It was found that the activation energy at the maximum of the TSL was equal to 0.235 and 0.250 eV for PMPSi doped with BNNI and BDNPH, respectively, that is higher value than 0.190 eV obtained for undoped PMPSi. Using these values one can obtain from the expression (3) $\sigma = 0.104$ and 0.110 eV for PMPSi + BNNI and PMPSi + BDNPH, respectively. These values are close to those obtained by the Gaussian analysis and agree quite well with the data obtained from the charge carrier transport measurements.

DISCUSSION

The quantum efficiency of the charge carrier photogeneration in PMPSi could be increased in the presence of chromophores both chemically bonded to the polymer backbone and simply added to the polymer. The increase in the photogeneration efficiency was related to electron affinity of the nitro groups present in the chromophore. It followed from the experiments made on PMPSi doped with various low-molecular-weight additives that the photogeneration efficiency increased with increasing electron affinity of the dopant.[10] In contrast, when PMPSi was substituted with chromophores bearing electron-donating dimethylamino groups, the photogeneration efficiency dropped considerably compared with that observed with undoped PMPSi, despite of the tail in the visible region of absorption spectrum similarly to the polymer PMPSi-DNPH.[8,9] This suggests that the photoinduced charge-transfer is an important step in the photogeneration process. To overcome the strong geminate recombination of the electron-hole pair photogenerated within the backbone, the electron must be transferred to polymer side group or to an electron acceptor in the vicinity of the polymer chain. The probability of the formation of an electron-hole pair within the chromophore can be considerably increased by migration of the excitation energy absorbed by the σ-conjugated electron system of the poly(silylene) backbone to the chromophore. The rapid decrease in the fluorescence intensity of PMPSi observed when BNNI and BDNPH were added, suggests that one chromophore molecule could quench fluorescence from many neighbouring methyl(phenyl)silylene repeating units.

The efficiency of an individual photogeneration centre decreases with increasing concentration of the chromophore due to a competition of energy/charge collecting centres. Thus, even an admixture of a small amount of the chromophore increased the primary photogeneration efficiency which, however, reached saturation and sometimes decreased with its increasing concentration. In addition, the photogenerated thermalized electron localized at the chromophore could act as a Coulomb-type recombination centre for free hole moving in the PMPSi matrix. At high chromophore concentrations, the apparent photogeneration efficiency calculated as an integral of the photocurrent transient may decrease due to an increased probability of recombination. An optimum chromophore concentration yielding the highest apparent photogeneration efficiency can, therefore, be found if both the photogeneration and recombination processes are balanced.

Saturation of the photogeneration efficiency with increasing electric field strength in sandwich-type samples is due to the barrier-limited current. Interestingly, the presence of acceptor groups, both chemically bonded to the backbone and admixed to the polymer, effectively decreased the barrier. Due to quite a high

absorption coefficient of the PMPSi at 347 nm the charges were generated only in a thin layer at the irradiated surface determined by the penetration depth of the incident light. Thus, the charge photogeneration in the sandwich samples could be strongly affected by an energetic barrier at the interface between PMPSi and the illuminated ITO electrode. The electric field dependence of the photogeneration efficiency could usually be fitted by the Onsager model of geminate recombination[28,29] for both PMPSi and PMPSi-DNPH if the non-contact xerographic discharge method[11] is used for the photoconductivity studies. However, in the low-field region, the barrier effect[22] prevailed (Figure 5, curves 1 and 2) for sandwich samples.

There are several models available for the description of the effect of additives on the charge carrier mobility in PMPSi. The multiple trapping of free holes by additive molecules was adopted for the explanation of the mobility decrease in PMPSi containing additives with ionisation potentials lower than that of PMPSi.[36] However, in our case, the decrease in the mobility caused by the presence of chromophores is related to the polar character of the chromophore.

An attempt was made[37] to employ a pure polaron model describing the charge carrier transport as a thermally activated hopping over energetic barriers modified with dipole relaxation in the vicinity of a momentarily localized charge. The equation

$$\mu = F^{-1} \sinh[\exp(edF/2kT)], \tag{4}$$

where e is the elementary charge and d is the hopping distance, was used by us to fit the mobility vs. electric field dependences measured in this work. However, our experimental data could not be fitted with the relation predicted by the polaron model only.

The observed negative slope of the field dependence of the mobility at the low field strengths and a linear log μ vs. $F^{1/2}$ dependence at high fields suggest that the charge carrier transport is influenced by localized hopping states distributed in energy and position.[35,38] The broadening of the energetic distribution of the transport states is illustrated by data in Table I. The half-width of the distribution, σ, decreased with increasing concentration of the chromophores. The parameter σ was determined from log μ vs. $F^{1/2}$ dependences measured in the high field region using the relation[35]

$$\ln \mu = \ln \mu_0 - (2\sigma/3\ kT)^2 + C\left[(\sigma/kT)^2 - \Sigma^2\right] F^{1/2}, \tag{5}$$

where μ_0 is the mobility in an ordered reference system, σ and Σ are parameters of the energetic and positional disorder, respectively, and C is a constant. The electric field dependences of μ measured at various temperatures were extrapolated to the zero field and values μ_0 and σ were calculated from the $\ln\mu(F\rightarrow 0)$ vs.

T^{-2} plot. The fitted lines (1 and 2) shown in Figure 4 demonstrate good linear fits of the dependences as predicted by the disorder model. However, at a high chromophore concentration, 10 mole %, a deviation of experimental data from the theoretical dependence could be seen (Figure 4, curve 3). The broadening of DOS distribution after doping was also demonstrated by the TSL technique. The agreement of the σ-parameters obtained from TOF and TSL experiments is quite good, (cf. σ for BNNI doped PMPSi from TSL, σ = 0.110 eV, 0.9 % BNNI, and σ from TOF experiments, σ = 0.107 eV, 1.7 % BNNI). However, not only the concentration but also the dipole moment of additive molecules is important. The higher the dipole moment, the broader was the distribution (higher σ – cf. Figure 7). The disorder model describes transport properties of PMPSi quite well.

TABLE I Parameters of charge carrier transport in poly(silylene)s

Polymer	*Chromophore concentration [mole %]*	μ_0 *[m^2/Vs]*	σ *[eV]*
PMPSi	0.00	1.2×10^{-6}	0.093
PMPSi – DNPH	0.55	1.2×10^{-6}	0.094
	0.88	1.0×10^{-6}	0.099
	1.29	1.1×10^{-6}	0.107
PMPSi + BNNI	0.43	0.9×10^{-6}	0.094
	1.74	0.5×10^{-6}	0.104
	3.59	1.6×10^{-6}	0.107

It could be pointed out that in this paper only the disorder model without the polaron contribution was taken into account. Nevertheless, this simplification could not qualitatively influence the mentioned relations. Quantitatively, the σ parameters are lower for the model including polaron contribution. The polaron binding energy for undoped PMPSi is $E_p = 0.16$ eV.[4] The polaron argument rests on the idea that the configuration of a hopping site is altered upon removal or addition of an extra electron. The motion of the carrier induces deformations along its path. A significant distortion of the PMPSi chain was recently found by Kim et al.[39] by measuring the migration rate of the excitation energy along the polymer chain. Taking into account the contributions both from the dynamic disorder, i.e. the polaronic barrier, and from the static disorder, i.e., the overall variation of the potential energy of the carrier as a result of the disordered environment, the effective zero-field activation energy of the mobility can be expressed by the relation

$$E^{\mu}_{aeff}(F \to 0) \approx E^{pol}_{a} + E^{dis}_{aeff} = \frac{E_p}{2} + \frac{8}{9}\frac{\sigma_p^2}{kT}, \qquad (6)$$

where E_a^{pol} and E_{aeff}^{dis} are the polaronic and disorder contributions, σ_p is the width of the DOS distribution (taking into account the polaron contribution). Since E_p reflects an intramolecular property, it is not influenced by the spatial distribution of hopping states. The zero-field value of the activation energy in PMPSi was $E_{aeff}^{dis}(F \to 0) = 0.30$ eV. The value of σ recalculated using Eq. (7)

$$\mu(T, F \to 0) \sim \exp[-(2\sigma/3kT)^2], \tag{7}$$

was 0.093 eV (at room temperature), taking into account the disorder model only. The real value of the width of the distribution of hopping sites σ would be lowered by the polaron contribution ($E_{aeff}^{dis} - E_p/2 = 8\sigma_p^2/9kT$, cf. Eq. 6). This leads to the value σ_p= 0.080 eV.

CONCLUSIONS

Both the chemical bonding and admixture of polar electron-acceptor chromophores in PMPSi were found to change the charge photogeneration and transport properties of the polymer. Whereas the charge carrier mobility decreased for any chromophore concentration used in the study, the photogeneration efficiency increased for small concentrations (up to 4 mole %) and decreased for higher concentrations. A maximum in the dependence of photogeneration efficiency vs. chromophore concentration exists due to a balance between the increasing effect of photogeneration and recombination centres with increasing chromophore concentration. At low chromophore concentrations (below 2 mole %), the photogeneration efficiency of free charge carriers increased by nearly one order of magnitude while the decrease in the hole mobility remained negligible. The effect of the decrease in the mobility is influenced by electron-dipole interactions and by broadening of DOS distribution.

Acknowledgements

The research reported in this paper was supported by the Grant Agency of the Academy of Sciences of the Czech Republic (grants No A1050901 and 12/96/K), by the Ministry of Education, Youth and Sports of the Czech Republic (grant Me 270/1999 KONTAKT), by Award No. UE1–326 of the U.S. CRDF, and in part within the Joint Project of the Polish-Ukrainian Scientific Cooperation.

References

(1) M. Fujino, *Chem. Phys. Lett.*, **136**, 451 (1986).
(2) M.A. Abkowitz, M. Stolka, R.J. Weagley, K.M. McGrane, and F.E. Knier, in Silicon – based Polymer Science, J. M. Zeigler and F. W. Gordon, (Eds.); *Adv. Chem. Ser.*, **224**, 467 (1990).
(3) L. M. Samuel, P. N. Sanda, and R. D. Miller, *Chem. Phys. Lett.*, **159**, 227 (1989).

(4) H. Bässler, P. M. Borsenberger, and R. J. Perry, *J. Polym. Sci., Polym. Phys.*, **32**, 1677 (1994).
(5) H. Suzuki, H. Meyer, S. Hoshino, and D. Haarer, *J. Appl. Phys.*, **78**, 2684 (1995).
(6) R. G. Kepler, J. M. Zeigler, L. A. Harrah and S. R. Kurtz, *Phys. Rev., B*, **35**, 2818–22 (1987).
(7) I. Kminek, E. Brynda, and W. Schnabel, *Eur. Polym. J.*, **227**, 1073 (1991).
(8) J. Pfleger, I. Kminek, S. Nešpůrek, and W. Schnabel, *IEEE Trans. Electr. Insul.*, **27**, 856 (1992).
(9) I. Kminek, S. Nešpůrek, E. Brynda, J. Pfleger, V. Cimrova, and W. Schnabel, *Collect. Czech. Chem. Commun.*, **58**, 2337 (1993).
(10) E. Brynda, S. Nešpůrek, and W. Schnabel, *Chem. Phys.*, **175**, 459 (1993).
(11) A. Eckhardt, V. Herden, S. Nešpůrek, and W. Schnabel, *Philos. Mag. B*, **71**, 239 (1995).
(12) X.-H. Zhang and R. West, *J. Polym. Sci.: Polym. Chem. Ed.*, **22**, 159 (1984).
(13) J. T. Ayres and C.K. Mann, *J. Polym. Sci., Polym. Lett. Ed.* **3**, 505 (1965).
(14) L. B. Schein, *Philos. Mag. B*, **65**, 795 (1992).
(15) H. Bässler, *Phys. Status Solidi B*, **175**, 15 (1993).
(16) I. A. Tale, *Phys. Status Solidi A*, **66**, 65 (1981).
(17) I. A. Tale, P.I. Butlers, S. Nešpůrek, and J. Pospíšil, *Izv. Akad. Nauk LatvSSR*, 40 (1987).
(18) P.I. Butlers, I. A. Tale, J. Pospíšil, S. Nešpůrek, *Prog. Coll. Polym. Sci.*, **78**, 93 (1988).
(19) A. Kadashchuk, N. Ostapenko, V. Zaika, and S. Nešpůrek, *Chem. Phys.*, **237**, 285,(1998).
(20) M. A. Abkowitz, F. E. Knier, H.-J. Yuh, R. J. Weagley, and M. Stolka, *Solid State Commun.*, **62**, 547 (1987).
(21) R. G. Kepler, J. M. Zeigler, L. A. Harrah, and S. R. Kurtz, *Phys. Rev. B*, **35**, 2819 (1982).
(22) V. Cimrova, S. Nešpůrek, R. Kužel, and W. Schnabel, *Synth. Met.*, **67**, 103 (1994).
(23) H. Bässler, in *Disorder Effects on Relaxational Processes* (R. Richert and A. Blumen Eds., Springer-Verlag, Berlin, Heidelberg, 1994), pp. 485–509.
(24) H. Bässler, *Phys. Status Solidi B*, **107**, 9 (1981).
(25) R. Eiermann, W. Hofberger, and H. Bässler, *J. Non-Cryst. Solids*, **28**, 415 (1978).
(26) A. Many and G. Rakavy, *Phys. Rev.*, **126**, 1980 (1962).
(27) R. G. Kepler, *Synth. Met.*, **28**, C 573 (1989).
(28) L. Onsager, *Phys. Rev.*, **54**, 554 (1938).
(29) S. Nešpůrek, V. Cimrová, J. Pfleger, and I. Kmínek, *Polym. Adv. Technol.*, **7**, 459 (1996).
(30) V. Cimrová, I. Kmínek, S. Nešpůrek and W. Schnabel, *Synth. Met.*, **64**, 271 (1994).
(31) S. Böhm, personal communication.
(32) H. Valerián, E. Brynda, S. Nešpůrek, and W. Schnabel, *J. Appl. Phys.*, **78**, 6071 (1995).
(33) A. Kadashchuk, N. Ostapenko, V. Zaika, P.M. Borsenberger, *J. Imag. Sci. Tech.*, **43**, 213 (1999).
(34) A. Kadashchuk, D.S. Weiss, P.M. Borsenberger, S. Nešpůrek, N. Ostapenko, V. Zaika, *Chem. Phys.*, **247**, 307 (1999).
(35) H. Bässler, *Phys. Status Solidi*, **175**, 15 (1993).
(36) K. Yokoyama and M. Yokoyama, *Solid State Commun.*, **73**, 199 (1990).
(37) A. V. Vannikov, A. Yu. Kryukov, A. G. Tyurin, and T. S. Zhuravleva, *Phys. Status Solidi A*, **115**, 47 (1989).
(38) P.M. Borsenberger and H. Bässler, *Phys. Status Solidi*, **170**, 291 (1992).
(39) Y. R. Kim, M. Lee, J. R. G. Thorne, R. M. Hochstrasser and J. M. Zeigler, *Chem. Phys. Lett.*, **145**, 75 (1988).